npj | Quantum Information

www.nature.com/npjqi

REVIEW ARTICLE OPEN

Majorana zero modes and topological quantum computation

Sankar Das Sarma[1,2], Michael Freedman[2] and Chetan Nayak[2,3]

We provide a current perspective on the rapidly developing field of Majorana zero modes (MZMs) in solid-state systems. We emphasise the theoretical prediction, experimental realisation and potential use of MZMs in future information processing devices through braiding-based topological quantum computation (TQC). Well-separated MZMs should manifest non-Abelian braiding statistics suitable for unitary gate operations for TQC. Recent experimental work, following earlier theoretical predictions, has shown specific signatures consistent with the existence of Majorana modes localised at the ends of semiconductor nanowires in the presence of superconducting proximity effect. We discuss the experimental findings and their theoretical analyses, and provide a perspective on the extent to which the observations indicate the existence of anyonic MZMs in solid-state systems. We also discuss fractional quantum Hall systems (the 5/2 state), which have been extensively studied in the context of non-Abelian anyons and TQC. We describe proposed schemes for carrying out braiding with MZMs as well as the necessary steps for implementing TQC.

npj Quantum Information (2015) **1,** 15001; doi:10.1038/npjqi.2015.1; published online 27 October 2015

INTRODUCTION

Topological quantum computation[1,2] is an approach to fault-tolerant quantum computation in which the unitary quantum gates result from the braiding of certain topological quantum objects called 'anyons'. Anyons braid non-trivially: two counter-clockwise exchanges do not leave the state of the system invariant, unlike in the cases of bosons or fermions. Anyons can arise in two ways: as localised excitations of an interacting quantum Hamiltonian[3] or as defects in an ordered system.[4,5] Fractionally charged excitations of the Laughlin fractional quantum Hall liquid are an example of the former. Abrikosov vortices in a topological superconductor are an example of the latter. Not all anyons are directly useful in topological quantum computation (TQC); only non-Abelian anyons are useful, which does not include the anyonic excitations (sometimes referred to as Abelian anyons, to distinguish them from the more exotic non-Abelian anyons, which are useful for TQC) that are believed to occur in most odd-denominator fractional quantum Hall states. A collection of non-Abelian anyons at fixed positions and with fixed local quantum numbers has a non-trivial topological degeneracy (which is, therefore, robust—i.e., immune to weak local perturbations). This topological degeneracy allows quantum computation as braiding enables unitary operations between the distinct degenerate states of the system. The unitary transformations resulting from braiding depend only on the topological class of the braid, thereby endowing them with fault tolerance. This topological immunity is protected by an energy gap in the system and a length scale discussed below. As long as the braiding operations are slow compared with the inverse of the energy gap and external perturbations are not strong enough to close the gap, the system remains robust to disturbances and noise. These braiding operations constitute the elementary gate operations for the evolution of the TQC.

Perhaps the simplest realisation of a non-Abelian anyon is a quasiparticle or defect supporting a Majorana zero mode (MZM). (The zero mode here refers to the zero-energy midgap excitations that these localised quasiparticles typically correspond to in a low-dimensional topological superconductor.) This is a real fermionic operator that commutes with the Hamiltonian. The existence of such operators guarantees topological degeneracy and, as we explain in section What is a majorana zero mode?, braiding necessarily causes non-commuting unitary transformations to act on this degenerate subspace. The term 'Majorana' refers to the fact that these fermion operators are real, as in Majorana's real version of the Dirac equation. However, there is little connection with Majorana's original work or its application to neutrinos. Rather, the key concept here is the non-Abelian anyon, and MZMs are a particular mechanism by which a particular type of non-Abelian anyons, usually called 'Ising anyons' can arise. By contrast, Majorana fermions, as originally conceived, obey ordinary Fermi–Dirac statistics, and are simply a particular type of fermion. Although the terminology 'Majorana fermions' is somewhat misleading for MZMs, it is used extensively in the literature.

If MZMs can be manipulated and their states measured in well-controlled experiments, this could pave the way towards the realisation of a topological quantum computer. The subject got a tremendous boost in 2012 when an experimental group in Delft published evidence for the existence of MZMs in InSb nanowires,[6] following earlier theoretical predictions.[7–9] The specific experimental finding, which has been reproduced later in other laboratories, is a zero-bias tunnelling conductance peak in a semiconductor (InSb or InAs) nanowire in contact with an ordinary metallic superconductor (Al or Nb), which shows up only when a finite external magnetic field is applied to the wire. Several other experimental groups also saw evidence (i.e., zero-bias tunnelling conductance peak in an applied magnetic field) for the existence of MZMs in both InSb and InAs nanowires,[10–14] thus verifying the Delft finding. However, though these experiments are compelling, they do not show exponential localisation with system length required by Eq. (3) or anyonic braiding behaviour. As explained later in this article, the exponential localisation of the isolated Majorana modes at wire ends and the associated non-Abelian braiding properties are the key features which enable TQC to be possible in these systems.

[1]Department of Physics, University of Maryland, College Park, MD, USA; [2]Microsoft Station Q, University of California, Santa Barbara, CA, USA and [3]Department of Physics, University of California, Santa Barbara, California, USA.
Correspondence: C Nayak (cnayak@microsoft.com)
Received 29 December 2014; revised 12 May 2015; accepted 12 May 2015

npj nature partner journals

In the current article, we provide a perspective on where this interesting and important subject is today (at the end of 2014). This is by no means a review article for the field of MZMs or the topic of TQC as such reviews will be too lengthy and too technical for a general readership. There are, in fact, several specialized review articles already discussing various aspects of the subject matter, which we mention here for the interested reader. The subject of TQC has been reviewed by us in great length earlier,[3] and we have also written a shorter version of anyonic braiding-based TQC elsewhere.[15] There are also several excellent popular articles on the braiding of non-Abelian anyons and TQC.[16,17] The theory of MZMs and their potential application to TQC have recently been reviewed in great technical depth in several articles.[18–21]

There are essentially two distinct physical systems that have been primarily studied in the search for MZMs for TQC. The first is the so-called 5/2-fractional quantum Hall system (5/2-FQHS) where the application of a strong perpendicular magnetic field to a very high-mobility two-dimensional (2D) electron gas (confined in epitaxially-grown GaAs–AlGaAs quantum wells) leads to the even-denominator fractional quantisation of the Hall resistance. The generic fractional quantum Hall effect leads to the quantisation with odd-denominator fractions (e.g., the original 1/3 quantisation observed in the famous experiment by Tsui *et al.*[22]). Interestingly, of the almost 100 FQHS states that have so far been observed in the laboratory, the 5/2-FQHS is the only even-denominator state ever found in a single 2D layer. It has been hypothesised that this even-denominator state supports Ising anyons. A topological qubit was proposed by us for this platform[23] in 2005, building upon previous theoretical work on the 5/2 state.[24–28] Tantalising experimental signatures for the possible existence of the desired non-Abelian anyonic properties were reported in subsequent experiments.[29–32] However, these results have not been reproduced in other laboratories. Potential barriers to progress are the required extreme high sample quality (mobility $>10^7$ cm^2/V.s), very low <25 mK temperature and high magnetic field >2 T. The second system is the semiconductor nanowire structure proposed in refs 7,8 building upon earlier theoretical work on topological superconductors.[33–36] Semiconductor nanowires are the focus of this paper, but the 5/2 fractional quantum Hall state is a useful point of comparison as a great deal of experimental and theoretical work has been done on the 5/2-FQHS over the last 27 years.

WHAT IS A MZM?

A MZM is a fermionic operator γ that squares to 1 (and, therefore, is necessarily self-adjoint) and commutes with the Hamiltonian H of a system:

$$\gamma \text{ fermionic}, \gamma^2 = 1, [H, \gamma] = 0 \tag{1}$$

Any operator that satisfies the first two conditions is called a Majorana fermion operator. If it satisfies the third condition, as well, then it is a MZM operator or, simply, a MZM. (For the experts, it might be useful to comment that propagating Majorana fermions, of the type that neutrinos are hypothesised to be, can occur in any superconductor. However, localised MZMs and their concomitant non-Abelian anyonic braiding is a much more remarkable phenomenon.) The existence of such operators implies the existence of a degenerate space of ground states, in which quantum information can be stored. If there are $2n$ MZMs, $\gamma_1,\ldots\gamma_{2n}$ (they must come in pairs as each MZM is, in a sense, half a fermion) satisfying

$$\{\gamma_i, \gamma_j\} = 2\delta_{ij} \tag{2}$$

then the Hamiltonian can be simultaneously diagonalised with the operators $i\gamma_1\gamma_2$, $i\gamma_3\gamma_4$, …, $i\gamma_{2n-1}\gamma_{2n}$. The ground states can be labelled by the eigenvalues ± 1 of these n operators, thereby leading to a 2^n-fold degeneracy. There is a two-state system associated with each pair of MZMs. This is to be contrasted with a collection of spin-1/2 particles, for which there is a two-state system associated with each spin. In the case of MZMs, we are free to pair them however we like; different pairings correspond to different choices of basis in the 2^n-dimensional ground-state Hilbert space.

Unfortunately, the preceding mathematics is too idealised for a real physical system. If we are fortunate, there can, instead, be self-adjoint Majorana fermion operators $\gamma_1,\ldots, \gamma_{2n}$ satisfying the anti-commutation relations (2) and

$$[H, \gamma_i] \sim e^{-x/\xi} \tag{3}$$

where x is a length scale mentioned in the introduction (which can be construed to be the separation between two MZMs in the pair) and discussed momentarily, and ξ is a correlation length associated with the Hamiltonian H. In the superconducting systems that will be discussed in the sections to follow, ξ will be the superconducting coherence length. All states above the 2^{n-1}-dimensional low-energy subspace have a minimum energy Δ. In order for the definition (3) to approach the ideal condition (1), it must be possible to make x sufficiently large that the right-hand side of Equation (3) approaches zero rapidly. This can occur if the operators γ_i are localised at points x_i (which we have not, so far, assumed). Then γ_i commutes or anti-commutes, up to corrections $\sim e^{-y/\xi}$, with, respectively, all local bosonic or fermionic operators that can be written in terms of electron creation and annihilation operators whose support is a minimum distance y from some point x_i. The effective Hamiltonian for energies much lower than Δ is a sum of local terms, which means that products of operators such as $i\gamma_i\gamma_j$ must have exponentially small coefficients $\sim e^{-|x_i-x_j|/\xi}$. (Terms that contain a single γ_i operator (and no other fermionic operators, since none are allowed in the low-energy theory) are not allowed, due to fermion parity conservation.) Consequently, the condition (3) then holds (although much of the current interest in MZM and TQC is focused on semiconductor nanowires, as proposed in refs 7–9 the possibility of combining SO-coupling and spin splitting with ordinary *s*-wave superconductivity to artificially create topological (spinless) *p*-wave superconductivity was actually first considered theoretically[37,38] in the context of ultracold fermionic cold atoms.) The number of MZM operators satisfying (3) must be even. Consequently, if we add a term to the Hamiltonian that couples a single zero-mode operator to the non-zero-mode operators, a zero-mode operator will remain as zero modes can only be lifted in pairs. Thus, the exponential 'protection' of the MZMs allowing their quantum degeneracy is enabled by the energy gap, which should be as large as possible for effective TQC operations. Thus, in a loose sense, two Majoranas together give a Dirac fermion, and these two MZMs must be far away from each other for the exponential topological protection to apply.

It is useful to combine the two MZMs into a single Dirac fermion $c=\gamma_1+i\gamma_2$. The two states of this pair of zero modes corresponds to the fermion parities $c^\dagger c=0,1$. Thus, if the total fermion parity of a system is fixed, then the degeneracy of $2n$ MZMs is 2^{n-1}-fold. This quantum degeneracy, arising from the topological nature of the MZMs, enables TQC to be feasible by braiding the MZMs around each other.

Such localised MZMs are known to occur in two related but distinct physical situations. The first is at a defect in an ordered state, such as a vortex in a superconductor or a domain wall in a one-dimensional (1D) system. The defect does not have finite energy in the thermodynamic limit and, therefore, it is not possible to excite a pair of such defects at finite-energy cost and pull them apart. However, by tuning experimental parameters (which involves energies proportional to the system size), such

defects can be created in pairs, thereby creating pairs of MZMs. The best example of this is a topological superconductor. Alternatively, there may be finite-energy quasiparticle excitations of a topological phase[3] that support zero modes. This scenario is believed to be realized in the $\nu = 5/2$ fractional quantum Hall states, where *charge-e*/4 excitations are hypothesised to support MZMs. Although the cases of defects in topological superconductors and quasiparticles in 'true' topological phases are closely related, there are some important differences, touched on later.

When two defects or quasiparticles supporting MZMs are exchanged while maintaining a distance greater than ξ, their MZMs must also be exchanged. As the γ_i operators are real, the exchange process can, at most, change their signs. Moreover, fermion parity must be conserved, which dictates that γ_1 and γ_2 must pick up opposite signs. Hence, the transformation law is:

$$\gamma_1 \to \pm\gamma_2, \gamma_2 \to \gamma_1 \tag{4}$$

The overall sign is a gauge choice. This transformation is generated by the unitary operator:

$$U = e^{i\theta} e^{\frac{\pi}{4}\gamma_1\gamma_2} \tag{5}$$

This is the braiding transformation of Ising anyons. Strictly speaking, Ising anyons have $\theta = \pi/8$. Other values of θ can occur if there are additional Abelian anyons attached to the Ising anyons, as is believed to occur in the $\nu = 5/2$ fractional quantum Hall state. In the case of defects, rather than quasiparticles, the phase θ will not, in general, be universal, and will depend on the particular path through which the defects were exchanged. We emphasize that this braiding transformation law follows from (i) the reality condition of the Majorana fermion operators $\gamma_{1,2}$, (ii) the locality of the MZMs and (iii) conservation of fermion parity. Therefore, an experimental observation consistent with such a braiding transformation is evidence that (i)–(iii) hold. This in turn is evidence that the defects or quasiparticles support MZMs satisfying the definition (3). Such a direct experimental observation of braiding has not yet happened in the laboratory.

In the case of quasiparticles in topological phases, braiding properties, as revealed through various concrete proposed interference experiments such as those proposed in refs 23,27,37,38 is, perhaps, the gold standard for detecting MZMs. However, in the case of defects in ordered states and, in particular, in the special case of MZMs in superconductors, a zero-bias peak (ZBP) in transport with a normal lead[39] and a 4π periodic Josephson effect[34] are also signatures, as discussed in section Signatures of MZMs in topological superconductors. Before discussing these in more detail in section Signatures of MZMs in topological superconductors, it may be helpful to discuss the differences between topological superconductors and true topological phases.

MZMS IN TOPOLOGICAL PHASES AND IN TOPOLOGICAL SUPERCONDUCTORS

As noted in the Introduction, Ising anyons can be understood as quasiparticles or defects that support MZMs. In the Moore–Read Pfaffian state[24,25] and the anti-Pfaffian state,[40,41] proposed as candidate non-Abelian states for the 5/2-FQHS, *charge-e*/4 quasiparticles are Ising anyons.[26,42–48] There is theoretical[28,49–56] and experimental[29–32,57–62] evidence that the $\nu = 5/2$ fractional quantum Hall state is in one of these two universality classes. However, there are also some experiments[63–66] that do not agree with this hypothesis. The non-Abelian statistics of quasiparticles at $\nu = 5/2$ has been reviewed in ref. 3 and would require a digression into the physics of the fractional quantum Hall effect. Hence, we do not elaborate on it here, other than to note that Ising-type fractional quantum Hall states are very nearly topological phases, apart from some deviations that are salient on higher-genus surfaces.[67] However, the electrical charge that is attached to Ising anyons enables their detection through charge transport experiments.[23,27,37,38] Ising anyons also occur in some lattice models of gapped, topologically-ordered spin liquids.[68,69] These are true topological phases in which the MZM operators are associated with finite-energy excitations of the system and do not have a local relation to the underlying spin operators, much less the electron operators, whose charge degree of freedom is gapped. This limits the types of effects (in comparison to the superconducting case) that could break the topological degeneracy implied by Equations (1) and (2).

MZMs also occur at defects in certain types of superconductors that form a subset of the class generally called 'topological superconductors'.[33,34,70] We discuss these in general terms in this section and then in the context of specific physical realisations in section `Synthetic' realization of topological superconductors.

Topological phases have some topological features and some ordinary non-topological features. However, the interplay between these two types of physics is even more central in topological superconductors. This is both 'bad' and 'good.' It is bad if the non-topological features represent an opportunity for error or lead to energy splittings that decohere desirable superpositions. It is good when they allow a convenient coupling to conventional physics, something we had better have available if we ever wish to measure the topological system. In topological phases, there is a trivial tensor product situation in which the topological and the ordinary degrees of freedom do not talk to each other. In this case, we do not have to worry that the latter induce errors in the former, but they also will not be useful in initialising or measuring the topological degrees of freedom. (As always, in discussing topological physics, we regard effects that diminish exponentially with length, frequency or temperature as unimportant. This is somewhat analogous to computer scientists classifying algorithms as polynomial time or slower. Clearly the power and even the constants can make a difference, but such a structural dichotomy is a useful starting point.) So, for example, if there are phonons in a system, their interaction with topological degrees of freedom causes a splitting of the topological degeneracy that vanishes as $e^{-L/\xi}$ at zero temperature,[67] so we would consider the system as essentially a tensor product, with the phonons in a separate factor. However, a topological superconductor is not a true topological phase but, rather, following the terminology of ref. 67 a fermion parity protected quasi-topological phase. The qualifier 'quasi' permits the existence of benign gapless modes as discussed above. With slightly more precision: an excitation is topological if its local density matrices cannot be produced to high fidelity by a local operator acting from one of the system's ground states. 'Quasi' permits low-energy excitations (below the gap) provided they are not 'topological'. These subgap excitations surely do exist in real topological superconductors: there will be phonons and there will be gapless excitations of the superconducting order parameter—both are Goldstone modes of broken symmetries (translation in the first case and U(1)-charge conservation in the second). (The reader may wonder why the now-so-famous Higgs mechanism fails to gap the Goldstone mode of broken U(1). The answer is the mismatch of dimensions, the gauge field roams three-dimensional space while the superconductor lives in either two- or one-dimension. In the former case, the interaction with the gauge field causes superconducting phase fluctuations to have dispersion $\omega \sim (q)^{1/2}$ while in the latter case $\omega \sim q$. In a bulk three-dimensional superconductor the gauge boson is indeed gapped out.) The more serious caveat is fermion parity protected. This is simultaneously a blessing and a curse for any project to compute with MZMs in superconductors. The blessing is that the basis states of the topological qubit have this precise interpretation: fermion parity. If we are willing to move into an unprotected

regime to measure them, MZMs can be brought together and their charge parity detected locally. Using more sophistication, one could keep the MZMs at topological separation and exploit the Aharonov–Casher effect to measure the charge parity encircled by a vortex. So this coupling will allow measurement by physics very well in hand. (It is less clear how to do this with, for instance, the computationally more powerful Fibonacci anyons.[3]) Measurement is crucial for processing quantum information with MZMs as the braid group representation for Ising anyons is a rather modest finite group: beyond input and output, distillation of quantum states is needed,[71] and this is measurement intensive. The curse is quasiparticle poisoning. A nearby electron can enter the system and be absorbed by a MZM, thereby flipping the fermion parity—i.e., flipping a qubit. The electrons' charge is absorbed by the superconducting condensate. This propensity of a topological superconductor to be poisoned (or equivalently, the fermion parity to flip in an uncontrolled manner) represents a salient distinction from the Moore–Read state proposed for the $\nu = 5/2$ fractional quantum Hall state. In the Moore–Read state, the vortices carry electric charge ($\pm e/4$) and fermions carry charge 0 or $\pm 1/2$. Consequently, there is an energy gap to bringing an electron from the outside into a $\nu = 5/2$-fractional quantum Hall effect fluid. Its fermion parity can be absorbed by a MZM (as in the case of a topologial superconductor), but there is no condensate to absorb its charge; instead, four disjoint *charge-e*/4 quasiparticles must be created with their attendant energy cost. It would be harder to poison a $\nu = 5/2$ fluid but also harder to discern its state and the signatures discussed in the next section are not available for non-Abelian FQHS states. Thus, one must choose between potentially better protection (5/2-fractional quantum Hall effect) or easier measurement (topological superconductor).

SIGNATURES OF MZMS IN TOPOLOGICAL SUPERCONDUCTORS

Owing to the superconducting order parameter, it is possible for an electron to tunnel directly into a MZM in a superconductor. Suppose there is a MZM γ at the origin $x = 0$ in a superconductor. Then, if we bring a metallic wire near the origin, electrons can tunnel from the lead to the superconductor via a coupling of the form

$$H_{\text{tun}} = \lambda\, c^{\dagger}(0)\gamma\, e^{-i\theta(0)/2} + \lambda^{*}\gamma\, c(0) e^{i\theta(0)/2} \tag{6}$$

where $c(0)$ is the electron annihilation operator in the lead. For simplicity, we have suppressed the spin index, which is a straightforward notational choice if the superconductor and the lead are both fully spin polarised. In the more generic case, the spin index must be handled with slightly more care. Here θ is the phase of the superconducting order parameter. Ordinarily, we would expect that it would be impossible for an electron, which carries electrical charge, to tunnel into a MZM, which is neutral as $\gamma = \gamma^{\dagger}$. However, the superconducting condensate (which is a condensate of Cooper pairs that breaks the U(1) charge conservation symmetry) can accommodate electrical charge, thereby allowing this process, which is a form of Andreev reflection. In the case of the Moore–Read Pfaffian quantum Hall state, however, this is not possible. In order for an electron to tunnel into an MZM, four *charge-e*/4 quasiparticles must also be created in order to conserve electrical charge. This can only happen when the bias voltage exceeds four times the charge gap.

In the case of a topological superconductor, the coupling (6), which seems like a drawback as compared with a topological phase, can actually be an advantage as it opens up the possibility of a simple way of detecting MZMs that does not involve braiding them. For at $T, V \ll \Delta$, the electrical conductivity from a 1D wire through a contact described by Equation (6) takes the form:[39,72–74]

$$G(V,T) = \frac{2e^2}{h} h(T/V, T/\Lambda^{*}) \tag{7}$$

where $h(0,0) = 1$ and Λ^{*} is a crossover scale determined by the tunnelling strength, $\Lambda^{*} \sim \lambda^{y}$, where the exponent y depends on the interaction strength in the 1D normal wire so that $y = 1/2$ for a wire with vanishing interactions. At low voltage and low temperature, the conductivity is $2e^2/h$, indicative of perfect Andreev reflection: each electron that impinges on the contact is reflected as a hole and charge $2e$ is absorbed by the topological superconductor. There is vanishing amplitude for an electron to be scattered back normally. Such a conductivity can occur for other reasons (see, e.g., refs 75,76), but they are non-generic and require some special circumstances and can, in principle, be ruled out by further experiments. Thus, the observation of perfect Andreev reflection, with the associated quantised conductance at zero bias, robust to parameter changes, is an indication of the presence of a MZM. In section Topological superconductors: experiments and interpretation, we discuss the extent to which this quantised tunnelling conductance associated with the zero-energy midgap Majorana modes has actually been observed in experiments.

A second probe of MZMs that is special to topological superconductors is the so-called fractional Josephson effect. When two normal superconductors are in electrical contact, separated by a thin insulator or a weak link, the dominant coupling between them at low temperatures is

$$H = -J\cos\theta \tag{8}$$

where θ is the difference in the phases of the order parameters of the two superconductors. It is periodic in θ with period 2π. The Josephson current is the derivative of this coupling with respect to θ; it, too, is periodic in θ with period 2π. The Josephson coupling is proportional to the square of the amplitude for an electron to tunnel from one superconductor to the other, $J \propto t^2$. However, when two topologial superconductors are in contact and there are MZMs on both sides of the Josephson junction, the leading coupling is:

$$H = -it\gamma_L\gamma_R \cos(\theta/2) \tag{9}$$

So long as $i\gamma_L\gamma_R = \pm 1$ remains fixed during the measurement, the Josephson current now has period 4π, rather than 2π as in non-topological superconductors. An observation of the 4π 'fractional' Josephson effect in alternating current (AC) measurements would be compelling evidence in favour of the existence of MZMs in a superconducting system. However, if $i\gamma_L\gamma_R = \pm 1$ can vary in order to find the minimum energy at each value of θ, then it will flip when $\cos(\theta/2)$ changes sign. Consequently, the current will have period 2π. The value of $i\gamma_L\gamma_R = \pm 1$ can change if a fermion is absorbed by one of the zero modes γ_L or γ_R. Such a fermion may come from a localised low-energy state or an out-of-equilibrium fermion excited above the superconducting gap. In order to use the Josephson effect to detect MZMs, an alternating current measurement must be done at frequencies higher than the inverse of the timescale for such processes.

This can be done through the observation of Shapiro steps.[10] When an ordinary Josephson junction is subjected to electromagnetic waves at frequency ω, a direct current (DC) voltage develops and passes through a series of steps $V_{\text{DC}} = n(h)/(2e)\omega$ as the current is increased. However, when there are MZMs at the junction, then the 4π periodicity discussed above translates to Shapiro steps $V_{\text{DC}} = n(h)/(e)\omega$. In essence, charge transport across a junction with MZMs is due to *charge e* rather than charge $2e$ objects, so the flux periodicity and voltage steps are doubled. In terms of conventional Shapiro steps, the odd steps should be missing,[10] but the experiment actually observes only one missing odd step. This simple picture of missing odd Shapiro steps, although physically plausible, may not be complete, and a complete theory for Shapiro steps in the presence of MZMs has not yet been formulated (see, however, ref. 77).

'SYNTHETIC' REALISATION OF TOPOLOGICAL SUPERCONDUCTORS

Before further discussing experimental probes of Ising anyons, we pause to discuss 'synthetic' realisations of topological superconductors because it will be useful to have concrete device structures in mind when we describe procedures for braiding non-Abelian anyons. 'Synthetic' systems are important because there is no known 'natural' system that spontaneously enters a topological superconducting phase. The A-phase of superfluid He-3 (ref. 78) and superconducting Sr_2RuO_4 (ref. 79) are hypothesised to possess some topological properties, but it is not known precisely how to bring these systems into topological superconducting phases that support MZMs, nor is it known precisely how to detect and manipulate MZMs in these systems.[80] There are also specific proposals for converting ultracold superfluid atomic fermionic gases into topological superfluids,[81] but experimental progress has been slow in the atomic systems because of inherent heating problems. However, topological superconductivity can occur in 'synthetic' systems[7,8,35,36,82–84] that combine ordinary non-topological superconductors with other materials, thereby facilitating interplay between superconductivity and other (explicitly, rather than spontaneously) broken symmetries.

The following single-particle Hamiltonian is a simple toy model for a topological superconducting wire,[34] which illustrates how MZMs can arise at the ends of a 1D wire:

$$H=\sum_i\left(-t\left[c_{i+1}^\dagger c_i+c_i^\dagger c_{i+1}\right]-\mu c_i^\dagger c_i+\Delta c_i c_{i+1}+\Delta^* c_{i+1}^\dagger c_i^\dagger\right) \tag{10}$$

Here the electrons are treated as spinless fermions that hop along a wire composed of a chain of lattice sites labelled as $i=1, 2,\ldots, N$. It is assumed that a fixed pair field $\Delta=|\Delta|e^{i\theta}$ is induced in the wire by contact with a three-dimensional superconductor through the proximity effect. To analyse this Hamiltonian, it is useful to absorb the phase of the superconducting pair field into the operators c_j and then to express them in terms of their real and imaginary parts: $e^{i(\theta)/(2)}c_j=a_{1,j}+ia_{2,j}$, $e^{-i(\theta)/(2)}c_j^\dagger=a_{1,j}-ia_{2,j}$. The operators $a_{1,j}$, $a_{2,j}$ are self-adjoint fermionic operators—$a_{1,j}^\dagger=a_{1,j}$, $a_{2,j}^\dagger=a_{2,j}$—i.e., they are Majorana fermion operators. They are (generically) not zero modes as they do not commute with the Hamiltonian but they enable us to elucidate the physics of this Hamiltonian as it can be written as:

$$H=\frac{i}{2}\sum_j\left[-\mu a_{1,j}a_{2,j}+(t+|\Delta|)a_{2,j}a_{1,j+1}+(-t+|\Delta|)a_{1,j}a_{2,j+1}\right] \tag{11}$$

Now, it is clear that there is a trivial gapped phase (an atomic insulator) centred about the point $|\Delta|=t=0$, $\mu<0$. The Hamiltonian is a sum of on-site terms $i|\mu|a_{1,j}a_{2,j}/2$, each of which has eigenvalue $-|\mu|/2$ in the ground state, with minimum excitation energy $|\mu|$. However, there is another gapped phase that includes the points $t=\pm|\Delta|$, $\mu=0$. At these points, the Hamiltonian is a sum of commuting terms, but they are not on site. Consider, for the sake of concreteness, the point $t=|\Delta|$, $\mu=0$. Then the Hamiltonian couples each site to its neighbours by coupling $a_{2,j}$ to $a_{1,j+1}$. As a result, we can form a set of independent two-level systems on the links of the chain. Each link is in its ground state $ia_{2,j}a_{1,j+1}=-1$. However, there are 'dangling' Majorana fermion operators at the ends of the chain because $a_{1,1}$ and $a_{2,N}$ do not appear in the Hamiltonian. They are MZM operators:

$$\{a_{1,1},a_{2,N}\}=[H,a_{1,1}]=[H,a_{2,N}]=0 \tag{12}$$

If we move away from the point $t=|\Delta|$, $\mu=0$, $a_{1,1}$ and $a_{2,N}$ will appear in the Hamiltonian and, as a result, they will no longer commute with the Hamiltonian. However, there will be a more complicated pair of operators that are exponentially localised at the ends of the chain and satisfy Equation (3). Thus, the 1D toy model describes a system with localised zero-energy Majorana excitations at the wire ends, which serve as the defects.

Very similar ideas hold in 2D,[33,70] where an *hc*/2*e* vortex in a fully spin-polarised *p*+*ip* superconductor supports a MZM. The 1D edge of such a 2D superconductor supports a chiral Majorana fermion:

$$S=\int \mathrm{d}x\ \mathrm{d}t\ \chi(i\partial_t+v\partial_x)\chi \tag{13}$$

where $\chi(x,t)=\chi^\dagger(x,t)$ and $\{\chi(x,t),\chi(x',t)\}=2\delta(x-x')$. When an odd number of vortices penetrate the bulk of the superconductor, the field χ has periodic boundary conditions, $\chi(x,t)=\chi(x+L,t)$, where L is the length of the boundary. Then, the allowed momenta are $k=2\pi n/L$ with $n=0,1,2,\ldots$ and the corresponding energies are $E_n=vk$. The $k=0$ mode is a MZM. If an even number of vortices penetrate the bulk of the superconductor, χ has anti-periodic boundary conditions, $\chi(x,t)=-\chi(x+L,t)$ and there is no zero mode because the allowed momenta are $k=(2n+1)\pi/L$. A vortex may be viewed as a very short edge in the interior of the superconductor, so that there is a large energy splitting between the $n=0$ mode and the $n\geqslant 1$ modes.

Although the toy model described above is not directly experimentally relevant, we can realise either a 1D or a 2D topological superconductor in an experiment, if we somehow induce spinless *p*-wave superconductivity in a metal in which a single spin-resolved band crosses the Fermi energy. This can be done with a Zeeman splitting that is large enough to fully spin polarise the system, but superconductivity has never been observed in such a system; if induced through the superconducting proximity effect, it is likely to be very weak as the amplitude of Cooper pair tunnelling from the superconductor into the ferromagnet would be very small. However, the surface state of a three-dimensional topological insulator[85–87] has such a band that can be exploited for these purposes.[36] Moreover, a doped semiconductor with a combination of spin-orbit coupling and Zeeman splitting leads, for a certain range of chemical potentials, to a single low-energy branch of the electron excitation spectrum in both 2D (ref. 36) and 1D systems.[7–9] In the former case, the Zeeman field must generically be in the direction perpendicular to the 2D system. In the presence of a superconductor, such a Zeeman splitting must be created by proximity to a ferromagnetic insulator, rather than with a magnetic field. The exception is a system in which the Rashba and Dresselhaus spin-orbit couplings balance each other.[82] In 1D, however, the Zeeman field can be created with an applied magnetic field, thus making a 1D semiconducting nanowire with strong spin-orbit coupling and superconducting proximity effect particularly attractive as an experimental platform for investigating MZMs. This idea[7–9] has been adapted by several experimental groups.[6,10–14]

In all of these cases, the electron's spin is locked to its momentum, rendering it effectively spinless. Such a situation has the added virtue that an ordinary *s*-wave superconductor can induce topological superconductivity[7–9,35,36,88,89] as the spin-orbit coupling mixes *s*-wave and *p*-wave components. An effective model for this scenario takes the following form:

$$H=\int \mathrm{d}x\left[\psi^\dagger\left(-\frac{1}{2m}\partial_x^2-\mu+i\alpha\sigma_y\partial_x+V_x\sigma_x\right)\psi+\Delta\psi_\uparrow\psi_\downarrow+\mathrm{h.c.}\right] \tag{14}$$

This model is in the topological superconducting phase when the following condition holds:[7–9] $V_x>(|\Delta|^2+\mu^2)^{1/2}$, i.e., when the Zeeman spin splitting V_x is larger than the induced superconducting gap Δ and the chemical potential μ—a situation that presumably can be achieved by tuning an external magnetic field B to enhance the Zeeman splitting. (Although much of the current interest in MZM and TQC is focused on semiconductor nanowires,

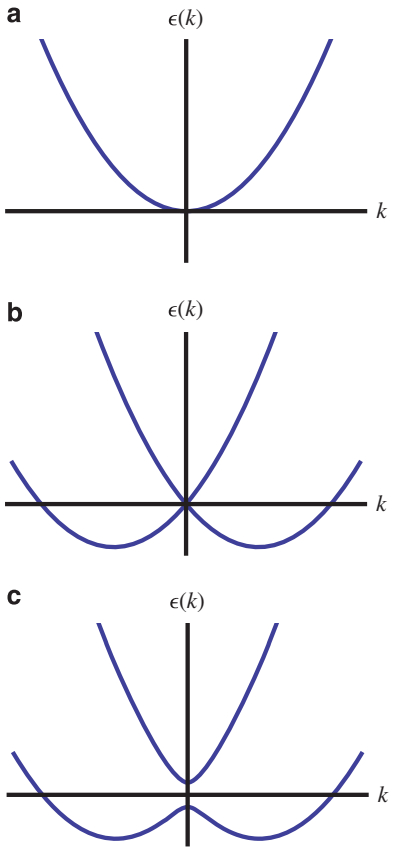

Figure 1. The electron energy $\varepsilon(k)$ as a function of momentum k for a 1D wire modelled by the Hamiltonian in Equation (14) for (**a**) vanishing spin-orbit coupling and Zeeman splitting; (**b**) non-zero spin-orbit splitting but vanishing Zeeman splitting; (**c**) non-zero spin-orbit and Zeeman splitting. In the situation in the **c**, if the Fermi energy is close to $\varepsilon = 0$, then there is effectively a single band of spinless electrons at the Fermi energy.

as proposed in refs 7–9 the possibility of combining spin-orbit-coupling and spin splitting with ordinary *s*-wave superconductivity to artificially create topological (spin less) *p*-wave superconductivity was actually first considered theoretically[91,92] in the context of ultracold fermionic cold atoms.) (In principle, the system can be tuned by changing the chemical potential as well using an external gate to control the Fermi level in a semiconductor nanowire, thus adding considerable flexibility to the set up for eventual TQC braiding manipulations of the MZMs.) When the two sides of this equation are equal, the system is gapless in the bulk and is at a quantum phase transition between ordinary and topological superconducting phases. The emergence of an effectively spinless band of electrons in this model is summarised by Figure 1. Here for simplicity, we have assumed that there is a single sub-band, i.e., a single transverse mode, in the wire. If there are more modes, then the requirement is that there must be an odd number of modes described by Equation (14) in the topological superconducting phase.[7,90,91] (In addition, there can be any number of modes in the non-topological phase; recall from section MZMs in topological phases and in topological superconductor that non-topological physics, here in the form of normal bands, may coexist with the topological bands.) From the preceding analysis, we see that there is a minimum magnetic field that must be exceeded in order for the system to be in a topological superconducting phase. In a real system in which there will be multiple sub-bands, there is a maximum applied magnetic field, too, beyond which the lowest empty sub-band

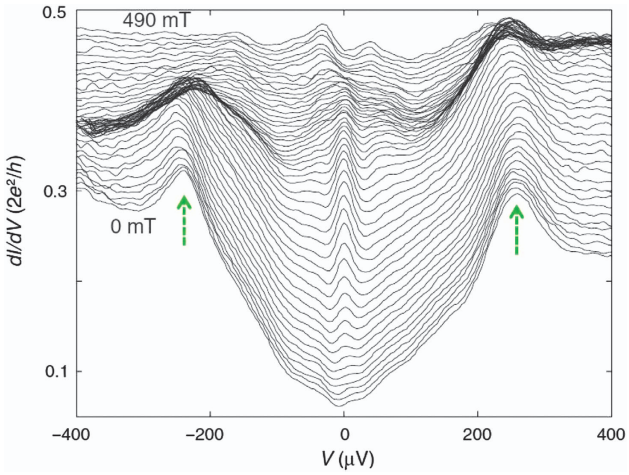

Figure 2. The experimental differential conductance spectrum in an InSb nanowire in the presence of a variable magnetic field showing the theoretically predicted Majorana ZBP at finite magnetic field (taken from ref. 6). See the text for a more detailed discussion of the experiment.

crosses the Fermi energy. (Also, at high applied fields, the topological superconducting gap decreases inversely with increasing spin splitting, thus requiring very low temperatures to study the MZMs.[9]) It is important that the magnetic field be perpendicular to the spin-orbit field. If the latter is in the *y*-direction, as in Equation (14), then the applied magnetic field must be in the $x-z$ plane. In practise, this angular dependence on the magnetic field can be and has been used to study the MZMs in the laboratory.[6]

TOPOLOGICAL SUPERCONDUCTORS: EXPERIMENTS AND INTERPRETATION

A number of experimental groups[6,10–14] have fabricated devices consisting of an InSb or InAs semiconductor nanowire in contact with a superconductor, beginning with the Mourik *et al.*[6] experiment. Both InSb and InAs have appreciable spin-orbit coupling and large Landé *g*-factor so that a small applied magnetic field can produce large Zeeman splitting. The experiments of refs 6,12 used the superconductor NbTiN, which has very high critical field, while the experiments of refs 11,13,14 used Al. All of these experiments observed a ZBP, consistent with the MZM expectation. The ZBP of Mourik *et al.*[6] is shown in Figure 2. Meanwhile, the experiment of ref.10 observed Shapiro steps in the alternating current Josephson effect in an InSb nanowire in contact with Nb.

According to the considerations of the previous two sections, once the magnetic field is sufficiently large that $V_x > (|\Delta|^2+\mu^2)^{1/2}$, where $V_x = g\mu_B B$, the conductance through the wire between a normal lead and a superconducting one will be $2e^2/h$ at vanishing bias voltage and temperature,[39,72–74] provided that the wire is much longer than the induced coherence length in the wire (i.e., the typical size of the localised MZMs). The five experiments of refs 6,11–14 observe a ZBP at magnetic fields $B \gtrapprox 0.1$ T, provided that the field is perpendicular to the putative direction of the spin-orbit field. The peak conductance is, however, significantly smaller than $2e^2/h$ in all of these experiments. Moreover, the wires appear to be short, as compared with the inferred coherence length in the wires, raising the question of why the MZM peak is not split into two peaks away from zero-bias voltage due to the hybridisation of the two end MZMs overlapping with each other (although some signatures of ZBP splitting are indeed observed in some of the data[6,11–14]). In addition, the subgap background conductance is

not very strongly suppressed at low non-zero voltages, i.e., the gap appears to be 'soft'. Finally, the appearance of the peak at $B \sim 0.1$ T does not appear to be accompanied by a closing of the gap, as expected at a quantum phase transition.

However, the peak conductance is expected to be suppressed by non-zero temperature in conjunction with finite tunnel barrier, and in short wires (see, e.g., refs 92,93). Some of the experiments do appear to find that the ZBP sometimes splits[12–14] and that this splitting oscillates with magnetic field, as predicted,[94] although a detailed quantitative comparison between experimental and theoretical ZBP splittings has not yet been carried out in depth, and such a comparison necessitates detailed knowledge about the experimental set ups (e.g., whether the system is at constant density or constant chemical potential[94]) unavailable at the current time. The softness of the gap may be due to disorder, especially inhomogeneity in the strength of the superconducting proximity effect[95] or perhaps an inverse proximity effect at the tunnel barriers where normal electrons could tunnel in from the metallic leads into the superconducting wire, leading to subgap states.[96] The softness of the gap may also help explain why the zero-bias conductance is suppressed from its expected quantised peak value, although other factors (e.g., finite wire length, finite temperature, finite tunnel barrier, etc.) are likely to be playing a role too. Very recent experimental efforts[97,98] using epitaxial superconductor (Al)-semiconductor (InAs) interfaces have led to hard proximity gaps. The absence of a visible gap closing at the putative quantum phase transition may be due to the vanishing amplitude of bulk states near the ends of the wire;[92] a tunnelling probe into the middle of the wire would then observe a gap closing (but presumably no MZM peaks that should decay exponentially with distance from the ends of the wires). Such a gap closing has been tentatively identified in the experiments on InAs nanowires in ref. 13.

In the experiment of ref. 10 it was observed that the $n=1$ Shapiro step was suppressed for magnetic fields larger than $B=2$ T. If this is the critical field beyond which $g\mu_B B_x = V_x > (|\Delta|^2+\mu^2)^{1/2}$ in this device, then all of the odd Shapiro steps should be suppressed. However, one could argue that the fermion parity of the MZMs fluctuates more rapidly at higher voltages so that only the $n=1$ step is suppressed. More theoretical work is necessary to understand Shapiro step behaviour in the presence of MZMs (see, however, ref. 77).

ZBPs can occur for other reasons, which must be ruled out before one can conclude that the experiments of refs 6,11–14 have observed a MZM, particularly as the expected conductance quantisation associated with the perfect Andreev reflection has not been seen. The Kondo effect leads to a ZBP.[75] In the presence of spin-orbit coupling and a magnetic field, the two-level system may not be the two states of a spin-1/2, but may be a singlet state and the lowest state of a triplet, which become degenerate at some non-zero magnetic field.[75] Alternatively, the ZBP may be due to 'resonant Andreev scattering'. Of course, a MZM is a type of resonant Andreev bound state so this alternative really means that there may be an Andreev bound state at the end of the wire that is not due to topological superconductivity but is 'accidentally' (i.e., at one point in parameter space, rather than across an entire phase) at zero energy. ZBPs could also arise simply due to strong disorder due to antilocalization at zero energy in 1D systems without time reversal, charge conservation or spin-rotational symmetry, usually called class D superconductors.[76]

The multiple observations of a ZBP in different laboratories, occurring only in parameter regimes consistent with theory[99–102] substantiate these interesting observations in semiconductor nanowires and show that they are, indeed, real effects and not experimental artifacts. Although these experiments are broadly consistent with the presence of MZMs at the ends of these wires, there is still room for scepticism, which can be answered by showing that the ZBPs evolve as expected when the wires are made longer, the soft gap is hardened (which has happened recently[97,98]), and the expected gap closing observed at the quantum phase transition. Finally, experiments that demonstrate the fractional alternating current Josephson effect and the expected non-Abelian braiding properties of MZMs would settle the matter.

Very recently, there has been an interesting new development: the claim of an observation of MZMs in metallic ferromagnetic (specifically, Fe) nanowires on superconducting (specifically, Pb) substrates where ZBPs appear at the wire ends without the application of any external magnetic field, presumably because of the large exchange spin splitting already present in the Fe wire.[103] There have been several theoretical analyses of this ferromagnetic nanowire Majorana platform[104–108] showing that such a system is indeed generically capable of supporting MZMs without any need for fine tuning of the chemical potential, i.e., the system is always in the topological phase as the spin splitting V_x is always much larger than Δ and μ. Although potentially an important development, more data (particularly, at lower temperatures, higher induced superconducting gap values and longer wires) would be necessary before any firm conclusion can be drawn about the experiment of ref. 103 as the current experiments, which are carried out at temperatures comparable to the induced topological superconducting energy gap in wires much shorter than the Majorana coherence length, only manifest very weak (3–4 orders of magnitude weaker than $2e^2/h$) and very broad (broader than the energy gap) ZBPs. If validated as MZMs, this new metallic platform gives a boost to the study of non-Abelian anyons in solid-state systems.

NON-ABELIAN BRAIDING

As noted in the introduction, the primary significance of MZMs is that they are a mechanism for non-Abelian braiding statistics, arising from their ground-state topological quantum degeneracy. The braiding of non-Abelian anyons provides a set of robust quantum gates with topological protection (although, of course, this only applies if the temperature is much lower than the energy gap and all anyons are kept much further apart than the correlation length, so that the system is in the exponentially small Majorana energy-splitting regime). These braiding properties are also the most direct and unequivocal way to detect non-Abelian anyons—including, as a special case, those supporting MZMs.

It is useful, at this point, to make a distinction between the two computational uses of braiding, for unitary gates and for projective measurement. Braiding-based gates can operate in essentially the same way for quasiparticles in a topological phase and for defects in an ordered (quasi-topological) state. However, braiding-based measurement procedures rely on interferometry, which is only possible if the motional degrees of freedom of the objects being braided are sufficiently quantum mechanical. This will be satisfied by quasiparticles at sufficiently low temperatures, but the motion of defects is classical at any relevant temperature except, possibly, in some special circumstances.

Consider, first, braiding-based gates. As noted above, braiding two anyons that support MZMs (either quasiparticles or defects) causes the unitary transformation in Equation (5). But how are we actually supposed to perform the braid? Here quasi-topological phases have an advantage over topological phases (which no one has presently proposed to build). In a true topological phase, it may be very difficult to manipulate a quasiparticle because it need not carry any global quantum numbers. However, in an Ising-type quantum Hall state, the non-Abelian anyons carry electrical charge, and one can imagine moving them by tuning electrical gates.[23] In the case of a 2D topological superconductor, MZMs are localised at vortices, and one can move vortices quantum mechanically through an array of Josephson junctions by tuning

fluxes. In a 1D topological superconducting wire MZMs are localised at domain walls between the topological superconductor and a non-topological superconductor or an insulator (e.g., at the wire ends). These domain walls can be moved by tuning the local chemical potential or magnetic field. In short, it is easier to 'grab' quasiparticles when they are electrically charged and, potentially, easier still to grab a defect when it occurs at a boundary between two phases between which the system can be driven by varying the electric or magnetic field.[109] The latter scenario is exemplified in Figure 3a. There are in fact many theoretical proposals on how to braid the end-localised MZMs using electrical gates in various *T* junctions made of nanowires, all of which depend on the ability of external gates in controlling semiconductor carriers. The potential to manipulate MZMs through external electrical gating is, in fact, one great advantage of semiconductor-based Majorana platforms.

In both cases, quasiparticles and defects, it turns out not to be necessary to move quasiparticles to braid them. Instead, one can effectively move non-Abelian anyons via a 'measurement-only' scheme.[110,111] Through the use of ancillary Einstein-Podolsky-Rosen (EPR) pairs and a sequence of measurements, quantum states can be teleported from one qubit to another. Similarly, a measurement involving an ancillary quasiparticle–quasihole or defect–anti-defect pair can be used to teleport a non-Abelian anyon. A sequence of such teleportations can be used to braid quasiparticles. The required sequence of measurements can be performed without moving the anyons at all, as illustrated by the flux-based scheme of refs 112–114. By tuning Josephson couplings (which can be done by varying the flux through SQUID loops), pairs of MZMs can be measured electrostatically, as depicted in Figure 3b. The fermion parity of a pair of MZMs is measured by isolating that pair on a small superconducting island so that the two parity states differ by an electrostatic charging energy. When the Josephson coupling between the island and a large superconductor is non-zero, that pair of MZMs is not measured, and a different pair (possibly involving one member of the first pair of MZMs) can be measured. Thereby, a measurement-only braiding scheme can be implemented without moving any defects at all; all that is necessary is to teleport their quantum information.

The second use of braiding is for interferometry-based measurement. This can only be done when the non-Abelian anyons are 'light' so that two different braiding paths can be interfered. This can be done with *charge-e*/4 quasiparticles in Ising-type $\nu = 5/2$ fractional quantum Hall states. The two-point contact interferometer depicted in Figure 4a measures the ratio between the unitary transformations associated with the two paths. In the case of non-Abelian anyons, this is not merely a phase. For Ising anyons, there is no interference at all when an odd number of MZMs is in the interference loop. When an even number is in the interference loop, the interference pattern is offset by a phase of 0 or π, depending on the fermion parity of the MZMs in the loop. The experiments of refs 29–32 are consistent with these predictions, but their interpretation has been questioned.[115]

Domain walls in nanowires are always classical objects whose position is determined by gate voltages. Abrikosov vortices in 2D topological superconductors are similarly classical in their motion. However, Josephson vortices, whose cores lie in the insulating barriers between superconducting regions, may move quantum mechanically, thereby making possible an interferometer such as that depicted in Figure 4. Moreover, the fermionic excitations at the edge of a superconductor are light and can be used to detect

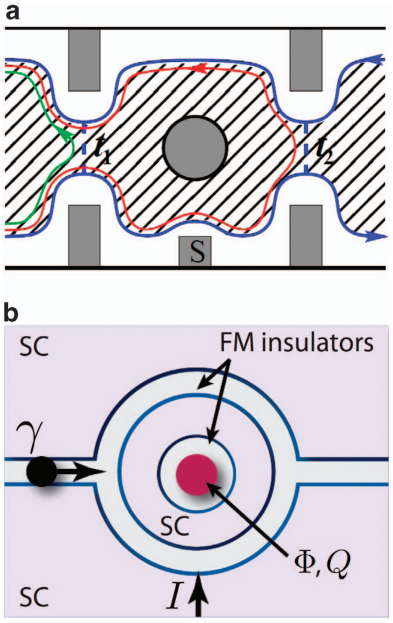

Figure 4. (**a**) With a two-point contact interferometer in a quantum Hall state, it is possible to detect topological charge and, thereby, read out a qubit by measuring electrical conductance (taken from ref. 3). (**b**) In a long Josephson junction with two arms, different paths for Josephson vortices can interfere, thereby enabling the detection of topological charge through electrical measurement (taken from ref. 18). Conversely, if two MZMs, 71 and 72, are brought close together, then the right-hand-side of Equation (3) may no longer be small.

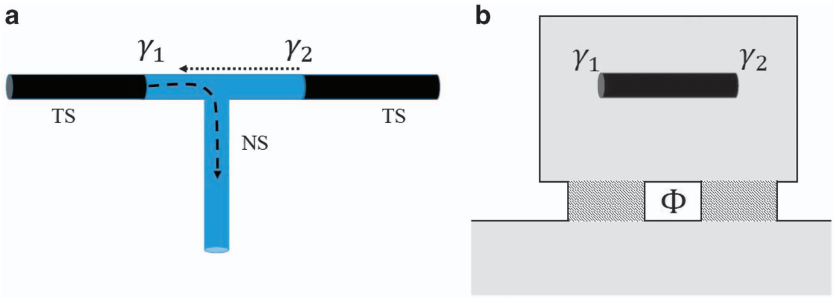

Figure 3. (**a**) MZMs localised at domain walls between topological superconducting (TS) and normal superconducting (NS) phases can be moved by tuning regions between these phases to move the domain walls.[109] (**b**) As explained in the text, a measurement-only scheme can replace actual movement of MZMs. A pair of MZMs can be measured by tuning the flux Φ through a SQUID loop to decouple the superconducting island on which the pair resides. This causes the island and nanowire to be in a superselection sector of fixed electrical charge.[112]

the presence or absence of a MZM (but not to detect the quantum information encoded in a collection of MZMs).

QUANTUM INFORMATION PROCESSING WITH MZMS

There are two primary approaches to storing quantum information in MZMs: 'dense' and 'sparse' encodings. In the dense encoding, n qubits are stored in $2n+2$ MZMs γ_1, γ_2,…, γ_{2n+2}. The two basis states of the k^{th} qubit correspond to the eigenvalues $i\gamma_{2k-1}\gamma_{2k}=\pm 1$. The last pair, γ_{2n+1}, γ_{2n+2} is entangled with the total fermion parity of the n qubits so that the state of the system is always an eigenstate of the total fermion parity of all $2n+2$ MZMs. The advantage of this encoding is that it is easy to construct gates that entangle qubits. The disadvantage is that the last pair of MZMs is always highly entangled with the rest of the system, so errors in that pair (even if rare) can infect all of the qubits. In the sparse encoding, n qubits are stored in $4n$ MZMs $\gamma_1,\gamma_2,\ldots,\gamma_{4n}$. For all k, we enforce the condition $\gamma_{4k-3}\gamma_{4k-2}\gamma_{4k-1}\gamma_{4k}=-1$, i.e., the total fermion parity of the set of four MZMs is even in the computational subspace. The two basis states of the k^{th} qubit correspond to the two eigenvalues $i\gamma_{4k-3}\gamma_{4k-2}=\pm 1$. (Note that, in the computational subspace, $i\gamma_{4k-3}\gamma_{4k-2}=i\gamma_{4k-1}\gamma_{4k}$.) As each quartet of MZMs has fixed fermion parity, it is easier to keep errors isolated. However, there are no entangling gates resulting from braiding alone. In order to entangle qubits, we need to perform measurements in order to pass from one encoding to the other.

The gates $H,T,\Lambda(\sigma_z)$ form a universal gate set, where H is the Hadamard gate, T is the $\pi/8$-phase gate and $\Lambda(\sigma_z)$ is the controlled-Z gate:

$$H=1\frac{}{\sqrt{2}}\begin{pmatrix}1 & 1\\ 1 & -1\end{pmatrix}, T=\begin{pmatrix}1 & 0\\ 0 & e^{i\pi/4}\end{pmatrix}, Z=\begin{pmatrix}1 & 0\\ 0 & -1\end{pmatrix}.$$

To apply the Hadamard gate to the k^{th} qubit, we perform a counterclockwise exchange of the MZMs γ_{4k-2} and γ_{4k-1}. In order to apply $\Lambda(\sigma_z)$ to two qubits encoded in eight MZMs, we first change to the dense encoding in which the two qubits are encoded in six MZMs. This involves a measurement. In this encoding, a braid implements $\Lambda(\sigma_z)$. Finally, we introduce an ancillary pair of MZMs and perform a measurement in order to return to the sparse encoding. To be more precise, suppose that our two qubits are associated with MZMs $\gamma_1,\ldots\gamma_8$ in the sparse encoding, with the first four encoding the first qubit and the second four the second qubit. First, we measure $i\gamma_4\gamma_5$. If it is equal to +1, then the remaining MZMs form a dense encoding of the two qubits. If the measurement returns -1, a straightforward correction will be needed. Then we perform a counterclockwise exchange 3 and 6 (which are the middle two of the remaining MZMs) followed by clockwise exchanges of 1 and 2 and of 7 and 8. Finally, we return to the sparse encoding by introducing an ancillary pair of MZMs, which we will call γ_4 and γ_5, which are in the known state $i\gamma_4\gamma_5=1$. Then a measurement of $\gamma_5\gamma_6\gamma_7\gamma_8$ returns the system to the sparse encoding.

A single-qubit phase gate can be performed by bringing two MZMs close together for a period of time, t, so that their two states will be split in energy by ΔE, and then pulling them apart again:

$$U=\begin{pmatrix}1 & 0\\ 0 & e^{i\Delta Et}\end{pmatrix} \quad (15)$$

This is a completely unprotected operation. Topology does not help us here. If we had perfect control over our system, then we would be able to control ΔE and t precisely so that we could set $\Delta Et=\pi/4$ and obtain a T gate. (Indeed, this is the type of control on which 'conventional' qubits rely.) However, we do not expect to have such perfect control, so some error correction will be needed. In the case of the T gate, for example, we can use 'magic state distillation'[71] to provide a higher fidelity T gate. Fortunately, the availability of topologically protected operations, namely protected Clifford operations, to perform error correction and distillation means fewer physical qubits should be required in the topological case compared with the conventional case.

The basic idea behind distillation is as follows. If we can produce the state $|a\rangle=|0\rangle+e^{i\pi/4}|1\rangle$ on demand, this is as good as being able to apply the T gate as we can perform a controlled-NOT (CNOT) gate with $|a\rangle$ as the control qubit and our data qubit as the target. This is followed by a measurement of the latter and a correction by a Clifford operation if the measurement returns a+1. Therefore, the goal is to produce a high-fidelity copy of $|a\rangle$. This can be done in a variety of ways and has become, now, highly optimised.[116–120]

The original distillation protocol[71,121] proceeds by taking 15 approximate copies of $|a\rangle$: $|\tilde{a}_1\rangle,\ldots,|\tilde{a}_{15}\rangle$, each with fidelity at least $1-\varepsilon$. The tensor product of these 15 states is projected on the code subspace of the[1,3,15] Reed–Muller code. This stabiliser code has the following properties: it encodes 1 logical qubit in 15 physical qubits; it can detect up to two phase (Z) errors and up to six bit (X) errors; and, remarkably, the logical state $|a\rangle$ is the product of 15 copies of $|a\rangle$. Consequently, given 15 noisy copies of $|a\rangle$, we can check 14 stabilisers to see if it is consistent with being in the Reed–Muller code subspace. If it is, we can decode the resulting 15 physical qubits into a logical qubit, which will be a purified version of the state $|a\rangle$, with fidelity $1-\varepsilon_{\text{out}}\approx 1-35\varepsilon^3$, in the limit that ε is small. Distillation improves the fidelity so long as the initial fidelity ε exceeds the threshold found by solving $\varepsilon_{\text{out}}(\varepsilon)=\varepsilon$. The threshold is roughly $\varepsilon_0\approx 0.141$ ref. 121. The distillation protocol can be applied recursively to achieve even higher fidelities on the state $|a\rangle$. Practically, the fidelity of the Clifford operations implementing the stabiliser checks dictates the minimum ε_{out} achievable using the distillation protocol. For example, to achieve $\varepsilon_{\text{out}}\approx 10^{-12}$, a reasonable value for quantum algorithms, the Clifford operations must also have fidelity of 10^{-12} (ref. 122) Conventional qubit systems will require, e.g., the surface code to achieve such fidelities on the Clifford operations, while topological qubit systems may achieve this fidelity naturally. Thus, a potential advantage of MZM-based TQC would be the need for fewer qubits and fewer gate operations than in conventional quantum computation.

A given quantum algorithm must be decomposed into a circuit consisting of gates drawn from a fault-tolerant universal gate set, such as the set consisting of $H,T,\Lambda(\sigma_z)$. Quantum algorithm decomposition methods based on algebraic number theory have recently dramatically reduced the number of T gates required to implement a given quantum algorithm.[123–125] By additionally allowing an ancilla qubit and measurement to be used during decomposition, another constant factor reduction in the number of T gates can be achieved.[126–128] The latter techniques are referred to as probabilistic 'Repeat-until-Success' circuits. These aforementioned methods, as well as, e.g., techniques to produce Fourier angle states,[129] may be ultimately hybridised to more efficiently and fault-tolerantly implement a quantum algorithm using Majorana anyons.

Before concluding this section, we briefly mention some of the potential problems in carrying out TQC with the current Majorana nanowire systems. First, the soft gap problem alluded to above indicates the presence of considerable non-thermal subgap fermionic states that would cause 'quasiparticle poisoning' of the MZM as the Majorana will hybridise with the subgap fermions and decay (and thereby lose its non-Abelian anyonic character). Thus, poisoning by stray subgap non-thermal quasiparticles puts an absolute upper bound on the effective Majorana coherence time as poisoning will directly destroy the fermion parity at the heart of the proposed non-Abelian TQC. Recent experimental work has suppressed quasiparticle poisoning considerably, leading to possible coherence times as long as 1 min.[130,131] Another issue is that the current experimental topological gap is rather small (a few K), whereas the Majorana splitting due to the overlap

of the MZMs from the two ends of the nanowire are likely to be in the range of 100–200 mK (as the current nanowires are rather short). The lack of a large separation between these two energy scales introduces complications as the TQC braiding operations must be slow ('adiabatic') compared with the topological gap energy and fast (so that one is in the topologically protected regime) compared with the Majorana splitting energy. Improvement in materials should lead to larger (smaller) gap (splitting), making this issue go away eventually. Finally, the current ZBPs, even assuming that they are indeed the predicted MZM conductance peaks, are much smaller (by more than an order of magnitude) than the quantised MZM conductance value of $2e^2/h$ associated with the Majorana-induced perfect Andreev reflection, perhaps because of finite temperature, short wire length and finite tunnel barrier at the interfaces. This could lead to severe visibility problem during Majorana braiding with very weak signal to noise ratio, necessitating considerable measurement averaging. Only future braiding experiments could actually decisively establish whether the observed ZBPs in the nanowire tunnelling measurements are indeed the predicted MZMs or not.

OUTLOOK

It does not seem fanciful to compare Majorana systems and non-Abelian topological quantum systems in general with the field-effect transistor (FET). Both are sweet theoretical solutions to the problem of efficient processing of signals and the information they carry. (For FETs, of course, this theoretical solution has turned out, through Moore's law, to be an astounding practical engineering success as well, leading to the modern information technology universe we live in.) The kinds of information (classical versus quantum) and the energy scales (eV versus meV) are different, just as the two ideas are temporally separated by more than 50 years, but each proposes a radical solution to an information processing roadblock. In each case, the roadblock was not absolute but sufficiently daunting to inspire serious and sustained effort. There were pretransistor electronic computers, and it may well be possible to build a pretopological quantum computer through an extraordinary investment in error correction using ordinary non-topological qubits.[132] As with our current efforts to build MZM systems, the history of the FET was anchored in materials development and required a rethinking of solid-state physics (involving substantial and continuous developments in surface science, semiconductor physics, materials growth and lithography). Today, building topological materials will push the frontiers of purity and precision in materials growth and force us to extend our ability to model exotic bulk materials, interfaces and, finally, devices. As our entire civilisation now turns around the transistor, it would be grandiloquent to claim any untested technology as the new transistor, and we make no such claim. No one can see the future. However, we have arrived at a gateway where, in the next few years, our ability to process information may explode disruptively; there is certainly a large heterogeneous international effort in this direction of building quantum information processing devices and circuits. In such a world the topological route is the analogue of the FET.

Edgar Lilienfeld filed the first FET patent in 1925. It was in an entirely metallic system in which the required electronic depletion was too difficult to accomplish reliably. It took roughly four decades and the advent of semiconductor devices to realise the initial FET vision. Where do we stand with MZM systems today? Experimentalists have picked the most promising materials: high Landé *g*-factor (to keep the applied *B*-fields moderate), high spin-orbit coupling (to strongly lock the spin and momentum bands in order to produce a large topological superconducting gap), low Schottky barriers and good epitaxial contact (to facilitate induced superconductivity), and high mobility (for coherent transport), among what was known, i.e., lying around, and predicted by the theorists. Incremental improvements in nanowire design, pacification of interfaces and transparency to contacting superconductors, may take us into the regime of workable devices—the transistor of the 1950s. But one may expect now that the concepts are clear, that systematic study of materials and their growth and interface properties could easily lead to new choices. A lesson already emerging from experiments in Copenhagen[97] can radically reduce subgap states. Their data shows a remarkably crisp Bardeen-Cooper-Schrieffer (BCS) spectrum in epitaxially coated nanowires.[98] We cannot of course be sure that the appropriate materials for the future TQC devices have already been developed—after all, the first transistors were made of germanium although silicon now rules the electronics world—but there is now a clear path for progress toward the eventual building of TQC using Majorana anyons.

The materials frontier discussed above addresses fidelity and lifetimes the numerator of the expression defining computational power. The denominator is the clock rate. In the case of a MZM system, the key timescale is that of measurement. As explained in section Quantum information processing with majorana zero modes, measurement of fermion parity is essential to the distillation of magic states and is the leading candidate even for braiding operations. To compute well we must be able to measure quickly and accurately. The two figures of merit are in fact related: if we can make n measurements within the qubit lifetime, it does us no good if the fidelity is $< 1 - 1/n$, for with less fidelity the qubit state will be forgotten long before we make the n^{th} measurement. For computations in parallel (as will be the norm), the demands on fidelity are proportionately greater because the appropriate n is the total number of measurements during the computation, not the number on any particular qubit. This tells us that there will be a second measurement frontier in which accuracy and speed will be the figures of merit. The leading measurement ideas today involve coupling to superconducting qubits living in an optical cavity and using a shift in the resonant frequency of the microwaves to read out fermion parity.[112,114] This is certainly a good starting point, but the typical number are photon frequencies ~6 GHz and, with beat frequencies recording the energy spitting of tens of MHz, read out would be limited to perhaps a MHz clock speed. The inherent energy scales of present MZM systems are on the order of 1 K≈20 GHz so there is room to do much better. In fact, to combine the two frontiers one might envision exploiting exotic superconductors with very large (~100 K) energy gap, pnictides or cuprates,[133,134] in conjuction with semiconductor wires to increase the gap protecting Majorana systems and clock rates by an order of magnitude.

Lifetimes/clock rate are hardware specs, but equally important is the scaling of the algorithms that we will run. There have been roughly three epochs: (i) Circa 1982, Feynman[135] told us that if we could build a quantum computer, its resource requirements would scale in precisely the same way as the quantum mechanical problems, e.g., quantum chemistry problems, we wished to solve—replacing the exponential scaling of a classical computer (in which memory must double to account for each new spin-1/2 degree of freedom); (ii) in the 1990s and 2000s, many key quantum algorithms were developed, including Shor's factoring algorithm,[136] and a detailed analysis of Feynman's idea; (iii) recent papers have focused on realistic regimes for quantum chemistry, rather than asymptotics. A straightforward estimate for gate counts of quantum chemistry Hamiltonians found that the number of computational steps for near equilibration to the ground-state scaled rather disastrously; polynomially by very high powers ~11 so that to obtain the energy of FeO_2 to a milliHartree with a GHz clock rate would take the age of the universe.[137] However, improved estimates,[138] combined with some algorithmic improvement,[139] has this time down now to a few minutes (with the most recent polynomial scaling ~5th power). This is one example; now that quantum computers appear to be increasingly

realistic, computer scientists and physicists will find efficient quantum algorthims for an array of problems. Many of these will be physical (e.g., quantum field theory[140] and many-body localisation are attractive targets[141]), but even areas distant from physics are seeing quantum advances. Deep learning has had a dramatic impact on machine learning in the last few years,[142–145] but there is a computational bottleneck: computation of the true gradient of L, where L is the 'log-likelihood function', is classically intractable, leading to classical methods that can efficiently only approximate ∇L. In physical terms, L is an entropy of a transverse field Ising model on a union of complete bipartite graphs. It is now known[146] that quantum computers may be used to estimate ∇L efficiently by emulating the corresponding Ising model, which leads to improved deep learning models using a quantum computer.

But when do we get to the analogue of the silicon FET? Presumably we will eventually do better than MZMs. Even as we anticipate great breakthroughs in the physics and engineering of Majorana systems, we can anticipate their eventual eclipse by anyonic systems (e.g., Fibonacci) that have topologically protected universal quantum operation. For many years, that phrase primarily meant a dense braid group representation. MZMs mirror the topological phase associated with $SU(2)_2$ (see, e.g., ref. 3 for an explanation of this notation). Fibonacci anyons are present in $SU(2)_3$ and have dense braid group representations. Furthermore, there is a hint of a potential path towards physical realisation[147] through a combination of fractional quantum Hall effect (at the $\nu = 2/3$ plateau) and superconductivity. SU(2) and all levels 5 and higher also have dense braiding but seem physically impractical. $SU(2)_4$ is an anomaly; it is potentially related to metaplectic anyonic systems[148] with a proposed realisation,[5,149–151] but braiding alone does not furnish a dense gate set. However, recent unpublished work[152] has demonstrated that $SU(2)_4$ becomes universal when braiding is combined with interferometric measurement.

We are poised on the brink of a revolution in our ability to control quantum systems. Topological systems, initially Majorana systems, will have a role. How wide the technological impact will be outside of physics is not foreseeable, but we can say that we are standing at a transition—we are about to learn to process information—to think, so to speak—in the manner that we know the universe operates: quantum mechanically. The first steps in this intellectual journey have been taken with the potential realisation of MZMs in the laboratory,[6,10–14] but we still have a long way to go.

REFERENCES

1 Kitaev AY. Fault-tolerant quantum computation by anyons. *Ann Phys (NY)* 2003; **303**: 2.
2 Freedman MH. P/NP, and the quantum field computer. *Proc Natl Acad Sci USA* 1998; **95**: 98.
3 Nayak C, Simon SH, Stern A, Freedman M, Sarma SD. Non-abelian anyons and topological quantum computation. *Rev Mod Phys* 2008; **80**: 1083.
4 Etingof P, Nikshych D, Ostrik V. Fusion categories and homotopy theory. *Quantum Topology* 2010; **1**: 209.
5 Barkeshli M, Bonderson P, Cheng M, Wang Z. Symmetry, defects, and gauging of topological phases. *Phys Rev X* 2014; **4**: 041035.
6 Mourik V, Zuo K, Frolov SM, Plissard SR, Bakkers EPAM, Kouwenhoven LP. Signatures of majorana fermions in hybrid superconductor-semiconductor nanowire devices. *Science* 2012; **336**: 1003.
7 Lutchyn RM, Sau JD, Das Sarma S. Majorana fermions and a topological phase transition in semiconductor-superconductor heterostructures. *Phys Rev Lett* 2010; **105**: 077001.
8 Oreg Y, Refael G, von Oppen F. Helical liquids and majorana bound states in quantum wires. *Phys Rev Lett* 2010; **105**: 177002.
9 Sau JD, Tewari S, Lutchyn RM, Stanescu TD, Das Sarma S. Non-Abelian quantum order in spin- orbit-coupled semiconductors: search for topological majorana particles in solid-state systems. *Phys Rev B* 2010; **82**: 214509.
10 Rokhinson LP, Liu X, Furdyna JK. The fractional a.c. Josephson effect in a semiconductor-superconductor nanowire as a signature of Majorana particles. *Nat Phys* 2012; **8**: 795–799.
11 Deng MT, Yu CL, Huang GY, Larsson M, Caroff P, Xu HQ. Anomalous zero-bias conductance peak in a nb–insb nanowire–nb hybrid device. *Nano Lett* 2012; **12**: 6414–6419.
12 Churchill HOH, Fatemi V, Grove-Rasmussen K, Deng MT, Caroff P, Xu HQ *et al*.. Superconductor-nanowire devices from tunneling to the multichannel regime: zero-bias oscillations and magnetoconductance crossover. *Phys Rev B* 2013; **87**: 241401.
13 Das A, Ronen Y, Most Y, Oreg Y, Heiblum M, Shtrikman H. Zero-bias peaks and splitting in an Al-InAs nanowire topological superconductor as a signature of Majorana fermions. *Nat Phys* 2012; **8**: 887–895.
14 Finck ADK, Van Harlingen DJ, Mohseni PK, Jung K, Li X. Anomalous modulation of a zero-bias peak in a hybrid nanowire-superconductor device. *Phys Rev Lett* 2013; **110**: 126406.
15 Das Sarma S, Freedman M, Nayak C. Topological quantum computation. *Phys Today* 2006; **59**: 32.
16 Venema L. Computing with quantum knots. *Sci Am* 2006; **294**: 56.
17 Venema L. Quantum computation: The dreamweaver's abacus. *Nature* 2008; **452**: 803–805.
18 Alicea J. New directions in the pursuit of Majorana fermions in solid state systems. *Rep Prog Phys* 2012; **75**: 076501.
19 Leijnse M, Flensberg K. Introduction to topological superconductivity and Majorana fermions. *Semicond Sci Technol* 2012; **27**: 124003.
20 Beenakker CWJ. Search for Majorana fermions in superconductors. *Annu Rev Condens Matter Phys* 2013; **4**: 113.
21 Stanescu TD, Tewari S. Majorana fermions in semiconductor nanowires: fundamentals, modeling, and experiment. *J Phys Condens Matter* 2013; **25**: 233201.
22 Tsui DC, Stormer HL, Gossard AC. Two-dimensional magnetotransport in the extreme quantum limit. *Phys Rev Lett* 1982; **48**: 1559–1562.
23 Das Sarma S, Freedman M, Nayak C. Topologically protected qubits from a possible non-Abelian fractional quantum Hall state. *Phys Rev Lett* 2005; **94**: 166802.
24 Moore G, Read N. Nonabelions in the fractional quantum Hall effect. *Nucl Phys B* 1991; **360**: 362–396.
25 Greiter M, Wen XG, Wilczek F. Paired Hall states. *Nucl Phys B* 1992; **374**: 567–614.
26 Nayak C, Wilczek F. 2*n*-quasihole states realize 2^{n-1} -dimensional spinor braiding statistics in paired quantum Hall states. *Nucl Phys B* 1996; **479**: 529–553.
27 Fradkin E, Nayak C, Tsvelik A, Wilczek F. A Chern-Simons effective field theory for the Pfaffian quantum Hall state. *Nucl Phys B* 1998; **516**: 704–718.
28 Morf RH. Transition from quantum Hall to compressible states in the second Landau level: new light on the $\nu = 5/2$ enigma. *Phys Rev Lett* 1998; **80**: 1505–1508.
29 Willett RL, Pfeiffer LN, West KW. Measurement of filling factor 5/2 quasiparticle interference with observation of charge e/4 and e/2 period oscillations. *Proc Natl Acad Sci USA* 2009; **106**: 8853–8858.
30 Willett RL, Pfeiffer LN, West KW. Alternation and interchange of e/4 and e/2 period interfer- ence oscillations consistent with filling factor 5/2 non-Abelian quasiparticles. *Phys Rev B* 2010; **82**: 205301 arXiv:09110345.
31 Willett RL, Pfeiffer LN, West KW, Manfra MJ. Aharonov–Bohm effect and coherence length of charge e/4 quasiparticles at 5/2 filling factor measured in multiple small Fabry–Perot interferometers (2013). unpublished data, arXiv:1301.2594.
32 Willett RL, Nayak C, Shtengel K, Pfeiffer LN, West KW. Magnetic-field-tuned Aharonov–Bohm oscillations and evidence for non-Abelian anyons at $\nu = 5/2$. *Phys Rev Lett* 2013; **111**: 186401.
33 Read N, Green D. Paired states of fermions in two dimensions with breaking of parity and time-reversal symmetries and the fractional quantum Hall effect. *Phys Rev B* 2000; **61**: 10267–10297.
34 Kitaev AY. QUANTUM COMPUTING: unpaired Majorana fermions in quantum wires. *Physics Uspekhi* 2001; **44**: 131.
35 Fu L, Kane CL. Superconducting proximity effect and Majorana fermions at the surface of a topological insulator. *Phys Rev Lett* 2008; **100**: 096407.
36 Sau JD, Lutchyn RM, Tewari S, Das Sarma S. Generic new platform for topological quantum computation using semiconductor heterostructures. *Phys Rev Lett* 2010; **104**: 040502.
37 Bonderson P, Kitaev A, Shtengel K. Detecting non-Abelian statistics in the $\nu = 5/2$ fractional quantum Hall state. *Phys Rev Lett* 2006; **96**: 016803.
38 Stern A, Halperin BI. Proposed experiments to probe the non-Abelian $\nu = 5/2$ quantum Hall state. *Phys Rev Lett* 2006; **96**: 016802.
39 Sengupta K, Zutic I, Kwon H-J, Yakovenko VM, Das Sarma S. Midgap edge states and pairing symmetry of quasi-one-dimensional organic superconductors. *Phys Rev B* 2001; **63**: 144531.
40 Lee S-S, Ryu S, Nayak C, Fisher MPA. Particle-hole symmetry and the $\nu = 5/2$ quantum Hall state. *Phys Rev Lett* 2007; **99**: 236807.

41 Levin M, Halperin BI, Rosenow B. Particle-hole symmetry and the Pfaffian state. *Phys Rev Lett* 2007; **99**: 236806.
42 Read N, Rezayi E. Quasiholes and fermionic zero modes of paired fractional quantum Hall states: the mechanism for non-Abelian statistics. *Phys Rev B* 1996; **54**: 16864–16867.
43 Tserkovnyak Y, Simon SH. Monte carlo evaluation of non-Abelian statistics. *Phys Rev Lett* 2003; **90**: 016802.
44 Seidel A. Pfaffian statistics through adiabatic transport in the 1d coherent state representation. *Phys Rev Lett* 2008; **101**: 196802.
45 Read N. Non-Abelian adiabatic statistics and Hall viscosity in quantum Hall states and $p_x + ip_y$ paired superfluids. *Phys Rev B* 2009; **79**: 045308.
46 Baraban M, Zikos G, Bonesteel N, Simon SH. Numerical analysis of quasiholes of the moore-read wave function. *Phys Rev Lett* 2009; **103**: 076801.
47 Prodan E, Haldane FDM. Mapping the braiding properties of the moore-read state. *Phys Rev B* 2009; **80**: 115121.
48 Bonderson P, Gurarie V, Nayak C. Plasma analogy and non-Abelian statistics for Ising-type quantum Hall states. *Phys Rev B* 2011; **83**: 075303.
49 Rezayi EH, Haldane FDM. Incompressible paired Hall state, stripe order, and the composite fermion liquid phase in half-filled Landau levels. *Phys Rev Lett* 2000; **84**: 4685–4688.
50 Feiguin AE, Rezayi E, Nayak C, Das Sarma S. Density matrix renormalization group study of incompressible fractional quantum hall states. *Phys Rev Lett* 2008; **100**: 166803.
51 Peterson MR, Jolicoeur T, Das Sarma S. Finitelayer thickness stabilizes the Pfaffian state for the 5/2 fractional quantum Hall effect: wave function overlap and topological degeneracy. *Phys Rev Lett* 2008; **101**: 016807.
52 Feiguin AE, Rezayi E, Yang K, Nayak C, Das Sarma S. Spin polarization of the $\nu = 5/2$ quantum hall state. *Phys Rev B* 2009; **79**: 115322.
53 Bishara W, Bonderson P, Nayak C, Shtengel K, Slingerland JK. The non-abelian interferometer. *Phys Rev B* 2009; **80**: 155303.
54 Rezayi EH, Simon SH. Breaking of particle-hole symmetry by landau level mixing in the $\nu = 5/2$ quantized hall state. *Phys Rev Lett* 2011; **106**: 116801.
55 Zaletel MP, Mong RSK, Pollmann F, Rezayi EH. Infinite density matrix renormalization group for multicomponent quantum Hall systems. *Phys Rev B* 2015; **91**: 045115.
56 Pakrouski K, Peterson MR, Jolicoeur T, Scarola VW, Nayak C, Troyer M. Phase diagram of the $\nu = 5/2$ fractional quantum Hall effect: effects of Landau-level mixing and nonzero width. *Phys Rev X* 2015; **5**: 021004.
57 Radu I, Miller J, Marcus C, Kastner M, Pfeiffer LN, West K. Quasiparticle properties from tunneling in the $\nu = 5/2$ fractional quantum hall state. *Science* 2008; **320**: 899–902.
58 Dolev M, Heiblum M, Umansky V, Stern A, Mahalu D. Observation of a quarter of an electron charge at the nu = 5/2 quantum Hall state. *Nature* 2008; **452**: 829.
59 Bid A, Ofek N, Inoue H, Heiblum M, Kane CL, Umansky V, Mahalu D. Observation of neutral modes in the fractional quantum Hall regime. *Nature* 2010; **466**: 585–590.
60 Venkatachalam V, Yacoby A, Pfeiffer L, West K. Local charge of the $\nu = 5/2$ fractional quantum Hall state. *Nature* 2011; **469**: 185–188.
61 Tiemann L, Gamez G, Kumada N, Muraki K. Unraveling the spin polarization of the $\nu = 5/2$ fractional quantum Hall state. *Science* 2011; **335**: 828–831.
62 Stern M, Piot BA, Vardi Y, Umansky V, Plo- chocka P, Maude DK, Bar-Joseph I. NMR probing of the spin polarization of the $\nu = 5/2$ quantum Hall state. *Phys Rev Lett* 2012; **108**: 066810.
63 Stern M, Plochocka P, Umansky V, Maude DK, Potemski M, Bar-Joseph I. Optical Probing of the spin polarization of the $\nu = 5/2$ quantum Hall state. *Phys Rev Lett* 2010; **105**: 096801.
64 Rhone TD, Yan J, Gallais Y, Pinczuk A, Pfeiffer L, West K. Rapid collapse of spin waves in nonuniform phases of the second Landau level. *Phys Rev Lett* 2011; **106**: 196805.
65 Lin X, Dillard C, Kastner MA, Pfeiffer LN, West KW. Measurements of quasiparticle tunneling in the $\nu = 5/2$ fractional quantum Hall state. *Phys Rev B* 2012; **85**: 165321.
66 Baer S, Roessler C, Ihn T, Ensslin K, Reichl C, Wegscheider W. Experimental probe of topological orders and edge excitations in the second Landau level. *Phys Rev B* 2014; **90**: 075403.
67 Bonderson P, Nayak C. Quasi-topological phases of matter and topological protection. *Phys Rev B* 2013; **87**: 195451.
68 Levin MA, Wen X-G. String-net condensation: a physical mechanism for topological phases. *Phys Rev B* 2005; **71**: 045110.
69 Kitaev AY. Anyons in an exactly solved model and beyond. *Ann Phys (NY)* 2006; **321**: 2–111.
70 Volovik GE. Fermion zero modes on vortices in chiral superconductors. *Soviet J Exp Theor Phys Letters* 1999; **70**: 609–614.
71 Bravyi S, Kitaev A. Universal quantum computation with ideal Clifford gates and noisy ancillas. *Phys Rev A* 2005; **71**: 022316.
72 Law KT, Lee PA, Ng TK. Majorana fermion induced resonant andreev reflection. *Phys Rev Lett* 2009; **103**: 237001.
73 Fidkowski L, Alicea J, Lindner NH, Lutchyn RM, Fisher MPA. Universal transport signatures of Majorana fermions in superconductor-Luttinger liquid junctions. *Phys Rev B* 2012; **85**: 245121.
74 Lutchyn RM, Skrabacz JH. Transport properties of topological superconductor-Luttinger liquid junctions: a real-time Keldysh approach. *Phys Rev B* 2013; **88**: 024511.
75 Lee EJH, Jiang X, Aguado R, Katsaros G, Lieber CM, Franceschi SDe. Zero-bias anomaly in a nanowire quantum dot coupled to superconductors. *Phys Rev Lett* 2012; **109**: 186802.
76 Bagrets D, Altland A. Class D spectral peak in Majorana quantum wires. *Phys Rev Lett* 2012; **109**: 227005.
77 Badiane DM, Glazman LI, Houzet M, Meyer JS. Ac Josephson effect in topological Josephson junctions. *Comptes Rendus Physique* 2013; **14**: 840–856.
78 Salomaa MM, Volovik GE. Half-quantum vortices in superfluid ^{3}He-*a*. *Phys Rev Lett* 1985; **55**: 1184–1187.
79 Mackenzie AP, Maeno Y. The superconductivity of *sr2ruo4* and the physics of spin-triplet pairing. *Rev Mod Phys* 2003; **75**: 657–712.
80 Das Sarma S, Nayak C, Tewari S. Proposal to stabilize and detect half-quantum vortices in Strontium Ruthenate thin films: Non-Abelian braiding statistics of vortices in a $p_x + ip_y$ superconductor. *Phys Rev B* 2006; **73**: 220502.
81 Tewari S, Das Sarma S, Nayak C, Zhang C, Zoller P. Quantum computation using vortices and Majorana zero modes of a $p_x + ip_y$ superfluid of fermionic cold atoms. *Phys Rev Lett* 2007; **98**: 010506.
82 Alicea J. Majorana fermions in a tunable semiconductor device. *Phys Rev B* 2010; **81**: 125318.
83 Potter AC, Lee PA. Multichannel generalization of Kitaev's Majorana end states and a practical route to realize them in thin films. *Phys Rev Lett* 2010; **105**: 227003.
84 Potter AC, Lee PA. Majorana end states in multiband microstructures with Rashba spin-orbit coupling. *Phys Rev B* 2011; **83**: 094525.
85 Moore JE, Balents L. Topological invariants of time-reversal-invariant band structures. *Phys Rev B* 2007; **75**: 121306.
86 Fu L, Kane CL, Mele EJ. Topological insulators in three dimensions. *Phys Rev Lett* 2007; **98**: 106803.
87 Roy R. Topological phases and the quantum spin hall effect in three dimensions. *Phys Rev B* 2009; **79**: 195322.
88 Zhang C, Tewari S, Lutchyn RM, Das Sarma S. $p_x + ip_y$ Superfluid from *s*-Wave Interactions of Fermionic Cold Atoms. *Phys Rev Lett* 2008; **101**: 160401.
89 Sato M, Takahashi Y, Fujimoto S. Non-Abelian topological order in *s*-wave superfluids of ultracold fermionic atoms. *Phys Rev Lett* 2009; **103**: 020401.
90 Lutchyn RM, Stanescu TD, Das Sarma S. Search for Majorana fermions in multiband semiconducting nanowires. *Phys Rev Lett* 2011; **106**: 127001.
91 Stanescu TD, Lutchyn RM, Das Sarma S. Majorana fermions in semiconductor nanowires. *Phys Rev B* 2011; **84**: 144522.
92 Stanescu TD, Tewari S, Sau JD, Das Sarma S. To close or not to close: the fate of the superconducting gap across the topological quantum phase transition in Majorana-carrying semiconductor nanowires. *Phys Rev Lett* 2012; **109**: 266402.
93 Lin C-H, Sau JD, Das Sarma S. Zero-bias conductance peak in Majorana wires made of semiconductor/superconductor hybrid structures. *Phys Rev B* 2012; **86**: 224511.
94 Das Sarma S, Sau JD, Stanescu TD. A Majorana smoking gun for the superconductor-semiconductor hybrid topological system. *ArXiv e-prints* 2012, 1211.0539.
95 Takei S, Fregoso BM, Hui H-Y, Lobos AM, Das Sarma S. Soft superconducting gap in semiconductor Majorana nanowires. *Phys Rev Lett* 2013; **110**: 186803.
96 Stanescu TD, Lutchyn RM, Das Sarma S. Soft superconducting gap in semiconductor-based Majorana nanowires. *Phys Rev B* 2014; **90**: 085302.
97 Krogstrup P, Ziino NLB, Chang W, Albrecht SM, Madsen MH, Johnson E *et al.* Epitaxy of semiconductor–superconductor nanowires. *Nat Mater* 2015; **14**: 400–406.
98 Chang W, Albrecht SM, Jespersen TS, Kuemmeth F, Krogstrup P, Nygard J*et al.* Hard gap in epitaxial semiconductor–superconductor nanowires. *Nat Nanotechnol* 2015; **10**: 232–236.
99 Brouwer PW, Duckheim M, Romito A, von Oppen F. Topological superconducting phases in disordered quantum wires with strong spin-orbit coupling. *Phys Rev B* 2011; **84**: 144526.
100 Brouwer PW, Duckheim M, Romito A, von Oppen F. Probability distribution of majorana end-state energies in disordered wires. *Phys Rev Lett* 2011; **107**: 196804.
101 Lobos AM, Lutchyn RM, Das Sarma S. Interplay of disorder and interaction in majo- rana quantum wires. *Phys Rev Lett* 2012; **109**: 146403.
102 Crepin Fmc, Zaránd G, Simon P. Nonperturbative phase diagram of interacting disordered majorana nanowires. *Phys Rev B* 2014; **90**: 121407.

103 Nadj-Perge S, Drozdov IK, Li J, Chen H, Jeon S, Seo J, MacDonald AH, Bernevig BA, Yazdani A. Observation of Majorana fermions in ferromagnetic atomic chains on a superconductor. *Science* 2014; **346**: 602–607.
104 Brydon PMR, Das Sarma S, Hui H-Y, Sau JD. Topological Shiba chain from spin-orbit coupling. *Phys Rev B* 2015; **91**: 064505.
105 Hui H-Y, Brydon PMR, Sau JD, Tewari S, Sarma SD. Majorana fermions in a ferromagnetic wire on the surface of a bulk spin-orbit coupled s-wave superconductor. *Sci Rep* 2015; **5**: 8880.
106 Li J, Chen H, Drozdov IK, Yazdani A, Bernevig BA, MacDonald AH. Topological superconductivity induced by ferromagnetic metal chains. *Phys Rev B* 2014; **90**: 235433.
107 Dumitrescu E, Roberts B, Tewari S, Sau JD, Das Sarma S. Majorana fermions in chiral topological ferromagnetic nanowires. *Phys Rev B* 2015; **91**: 094505.
108 Peng Y, Pientka F, Glazman LI, von Oppen F. Strong localization of Majorana end states in chains of magnetic adatoms. *Phys Rev Lett* 2015; **114**: 106801.
109 Alicea J, Oreg Y, Refael G, von Oppen F, Fisher MPA. Non-Abelian statistics and topological quantum information processing in 1D wire networks. *Nat Phys* 2011; **7**: 412–417.
110 Bonderson P, Freedman M, Nayak C. Measurement-only topological quantum computation. *Phys Rev Lett* 2008; **101**: 010501.
111 Bonderson P, Freedman M, Nayak C. Measurement-only topological quantum computation via anyonic interferometry. *Ann Phys* 2009; **324**: 787.
112 Hyart T, van Heck B, Fulga IC, Burrello M, Akhmerov AR, Beenakker CWJ. Flux-controlled quantum computation with Majorana fermions. *Phys Rev B* 2013; **88**: 035121.
113 Akhmerov AR, Nilsson J, Beenakker CWJ. Electrically detected interferometry of Majorana fermions in a topological insulator. *Phys Rev Lett* 2009; **102**: 216404.
114 Hassler F, Akhmerov AR, Hou C-Y, Beenakker CWJ. Anyonic interferometry without anyons: how a flux qubit can read out a topological qubit. *N J Phys* 2010; **12**: 125002.
115 Rosenow B, Halperin BI, Simon SH, Stern A. Exact solution for bulk-edge coupling in the non-Abelian $\nu = 5/2$ quantum Hall interferometer. *Phys Rev B* 2009; **80**: 155305.
116 Paetznick A, Reichardt B. Universal fault-tolerant quantum computation with only transversal gates and error correction. *Phys Rev Lett* 2013; **111**: 090505.
117 Jones C. Novel constructions for the fault-tolerant toffoli gate. *Phys Rev A* 2013; **87**: 022328.
118 Eastin B. Distilling one-qubit magic states into toffoli states. *Phys Rev A* 2012; **87**: 032321.
119 Bravyi S, Haah J. Magic state distillation with low overhead. *Phys Rev A* 2012; **86**: 052329.
120 Meier A, Eastin B, Knill E. Magic-state distillation 'with the four-qubit code, http://arxiv.org/abs/1204.4221.
121 Bravyi S. Universal quantum computation with the $\nu = 5/2$ fractional quantum Hall state. *Phys Rev A* 2006; **73**: 042313.
122 Brooks P. *Quantum error correction with biased noise*. Ph.D. thesis, California Institute of Technology 2013. http://resolver.caltech.edu/CaltechTHESIS:05302013-143644943.
123 Selinger P. Efficient Clifford+T approximation of single-qubit operators, http://arxiv.org/abs/1212.6253.
124 Kliuchnikov V, Maslov D, Mosca M. Fast and efficient exact synthesis of single qubit unitaries generated by clifford and T gates. *Quantum Inf Comput* 2013; **13**: 607–630.
125 Ross N, Selinger P. Optimal ancilla-free clifford+T approximation of *z*-rotations, arXiv:1403.2975. http://arxiv.org/abs/1403.2975.
126 Paetznick A, Svore K. Repeat-until-success: Non-deterministic decomposition of single-qubit unitaries. *Quantum Inf Comput* 2014; **14**: 1277.
127 Bocharov A, Roetteler M, Svore KM. Efficient synthesis of universal repeat-until-success circuits. arXiv:1404.5320.
128 Bocharov A, Roetteler M, Svore KM. Efficient synthesis of probabilistic quantum circuits with fallback. arXiv:1409.3552.
129 Duclos-Cianci G, Poulin D. Reducing the quantum computing overhead with complex gate distillation. arXiv:1403.5280.
130 van Woerkom DJ, Geresdi A, Kouwen- hoven LP. *ArXiv e-prints* 2015, 1501.03855. [153].
131 Higginbotham AP, Albrecht SM, Kirsanskas G, Chang W, Kuemmeth F, Krogstrup P, Jes TS. persen, J. Nygard, K. Flensberg, and C. M. Marcus. *ArXiv e-prints* 2015, 1501.05155.
132 Nielsen MA, Chuang IL. *Quantum Computation and Quantum Information*. Cambridge University Press: Cambridge, UK, 2000.
133 Kim Y, Cano J, Nayak C. Majorana zero modes in semiconductor nanowires in contact with higher-T_c superconductors. *Phys Rev B* 2012; **86**: 235429, 1208.3701.
134 Takei S, Fregoso BM, Galitski V, Das Sarma S. Topological superconductivity and Majorana fermions in hybrid structures involving cuprate high-T_c superconductors. *Phys Rev B* 2013; **87**: 014504.
135 Feynman RP. Simulating physics with computers. *Int J Theor Phys* 1982; **21**: 467–468.
136 Shor PW. Algorithms for quantum computation: Discrete logs and factoring. In: Shafi, G (ed.) *Proc. 35nd Annual Symposium on Foundations of Computer Science*. IEEE Computer Society Press: Los Alamitos, CA, USA, 1994, pp 124–134.
137 Wecker D, Bauer B, Clark BK, Hastings MB, Troyer M. Gate-count estimates for performing quantum chemistry on small quantum computers. *Phys Rev A* 2014; **90**: 022305.
138 Poulin D, Hastings MB, Wecker D, Wiebe N, Doherty AC, Troyer M. The trotter step size required for accurate quantum simulation of quantum chemistry. 2014, arXiv:1406.4920.
139 Hastings MB, Wecker D, Bauer B, Troyer M. Improving quantum algorithms for quantum chemistry. 2014, arXiv:1403.1539.
140 Jordan SP, Lee KSM, Preskill J. Quantum algorithms for quantum field theories. *Science* 2012; **336**: 1130.
141 Bauer B, Nayak C. Localization with a quantum computer. *Phys Rev X* 2014; **4**: 041021.
142 Hinton G, Osindero S, Teh Y-W. A fast learning algorithm for deep belief nets. *Neural Comput* 2006; **18**: 1527–1554.
143 Collobert R, Weston J. A unified architecture for natural language processing: deep neural networks with multitask learning. In: *Proc 25th International Conference on Machine Learning*. ACM, New York, NY, USA, 2008, 160–167.
144 Bengio Y. Learning deep architectures for AI. *Foundations Trends Machine Learning* 2009; **2**: 1–127.
145 LeCun Y, Kavukcuoglu K, Farabet C. Convolutional networks and applications in vision. In: *Circuits and Systems (ISCAS), Proc 2010 IEEE International Symposium on*. IEEE, Los Alamitos, CA, USA, 2010, 253–256.
146 Wiebe N, Kapoor A, Svore KM. Quantum deep learning. 2014, in preparation.
147 Mong RSK, Clarke DJ, Alicea J, Lindner NH, Fendley P, Nayak C, Oreg Y, Stern A, Berg E, Shtengel K *et al*. Universal topological quantum computation from a superconductor-abelian quantum Hall Heterostructure. *Phys Rev X* 2014; **4**: 011036.
148 Hastings MB, Nayak C, Wang Z. Metaplectic anyons, Majorana zero modes, and their compu- tational power. *Phys Rev B* 2013; **87**: 165421.
149 Clarke DJ, Alicea J, Shtengel K. Exotic non-abelian anyons from conventional fractional quantum Hall states. *Nat Commun* 2013; **4**: 1348.
150 Lindner NH, Berg E, Refael G, Stern A. Fractionalizing Majorana fermions: non-Abelian statistics on the edges of abelian quantum Hall states. *Phys Rev X* 2012; **2**: 041002.
151 Barkeshli M, Jian C-M, Qi X-L. Twist defects and projective non-abelian braiding statistics. *Phys Rev B* 2013; **87**: 045130.
152 Levaillant C, Bonderson P, Bauer B, Freed-man M unpublished data.